






## Fragmentation process of soil aggregates under concentrated water flow in red soil hilly region with different land use patterns

WEN Li-li<sup>1</sup>  <https://orcid.org/0009-0009-5682-9268>; e-mail: wenlili2017@163.com

WANG Jin-yue<sup>1</sup>  <https://orcid.org/0000-0003-3689-2533>; e-mail: wangjinyue2020@163.com

DENG Yu-song<sup>1</sup>  <https://orcid.org/0000-0002-9596-4413>; e-mail: denny2018@gxu.edu.cn

DUAN Xiao-qian<sup>2\*</sup>  <https://orcid.org/0000-0002-3157-6227>;  e-mail: duanxq2020@163.com

\*Corresponding author

<sup>1</sup> Guangxi Key Laboratory of Forest Ecology and Conservation, College of Forestry, Guangxi University, Nanning 530004, China

<sup>2</sup> Guangxi Key Laboratory of Agricultural environment and Agricultural product safety, College of Agriculture, Guangxi University, Nanning 530004, China

**Citation:** Wen LL, Wang JY, Deng YS, et al. (2023) Fragmentation process of soil aggregates under concentrated water flow in red soil hilly region with different land use patterns. *Journal of Mountain Science* 20(11). <https://doi.org/10.1007/s11629-023-8154-y>

© Science Press, Institute of Mountain Hazards and Environment, CAS and Springer-Verlag GmbH Germany, part of Springer Nature 2023

**Abstract:** The hilly area of red soil in the central subtropical region of China has a long history of severe soil erosion due to its abundance of water, heat, and intense agricultural and forestry activities. The Sandshale red soil area is hot and rainy, the local land utilization rate and replanting index are high, and the soil easily weathers and erodes, resulting in infertile and sandy soils, extensive soil erosion and large erosion, with far-reaching impacts. In this study, the stability of soil aggregates was studied by the wet sieving method and Le Bissonais (LB) method in six land use patterns in the Sandshale red soil area, including natural forest (NF), *Pinus massoniana* (PM), *Eucalyptus urophylla* × *E. grandis* (EU), orchard (OR), wasteland (WL) and arable land (AL). The transport damage characteristics of the soil aggregates under concentrated water flow were analyzed by using the soil aggregates to simulate the soil surface roughness in the field using a steel scouring flume with a variable slope. The results showed that: (1) the total soil porosity of the natural

forest was the highest, with 56.51% in A layer, which was 4.99% higher than the B layer, and the organic matter content ranged from 10.69 to 29.94 g.kg<sup>-1</sup> and was highest in NF and lowest in AL; (2) the maximum mean weight diameter (MWD) obtained by the wet sieving method was 4.81 mm for natural forest, and the MWD was the lowest in OR and AL at 2.45-2.77 mm. The MWD measured by the LB method was also highest in NF and lowest in AL. The contents of Fe<sub>a</sub> and Al<sub>a</sub> have a strong correlation with the stability parameters of soil aggregates; (3) the  $W_r/W_i$  results for the six land use patterns were NF>PM>EU>WL>OR>AL; the NF had the strongest soil aggregate stability, followed by WL, PM and EU, and AL and OR had the weakest; the stability of soil aggregates gradually weakened as the soil depth increased. Comprehensive analysis shows that forest land has high soil stability and obvious advantages in soil erosion resistance. Strengthening the construction of artificial forests can be an important means to reduce soil erosion in red soil hilly region.

**Received:** 09-Jun-2023

**Revised:** 27-Sep-2023

**Accepted:** 24-Oct-2023

**Keywords:** Soil aggregates; Land use; Aggregate stability; Fragmentation process

## 1 Introduction

Land degradation caused by soil erosion accounts for approximately 83% of all degraded land on Earth (Wang et al. 2009; Reza et al. 2018; Amézketa 1999). Soil erosion has become an important social and environmental problem currently because of its wide extent and large erosion volume, which produces serious hazards and has far-reaching effects (Tang et al. 2015).

Soil aggregates, as important structural units of soil, govern the various processes of material circulation and energy flow occurring in the soil. The composition, particle size and stability of soil aggregates influence soil erosion resistance, soil nutrient retention and conversion, etc. Moreover, they play very important roles in controlling the biological, chemical and physical properties of the soil (Jastrow 1996; Jastrow and Miller 1996; Wang et al. 2013a). Soil aggregates are structural units ranging in particle size from 0.25 to 10 mm formed by the cohesive bonding of soil particles (which contain soil microaggregates) (Wei and Bin 2002; Kalhor et al. 2017; Lu et al. 2016). Meanwhile, the aggregate stability can be used to quantify the quality condition of the soil, as some researchers point out that soil aggregate agglomeration and stability are the most important physical properties that influence and determine soil erodibility (Ewing and Mitchell 1986; Dexter 1991; An et al. 2013). Tisdall and Oades (1982) proposed a “hierarchical development model of aggregates” based on the different sizes of structural units in soil aggregates. The model describes that aggregates are formed by cementing microaggregates to small aggregates and then small aggregates to large aggregates in a stepwise manner. The soil mucilage content, which is the cementing material, determines the texture of the soil and plays an important role in the formation of aggregates (Curtin et al. 1994). It is generally accepted that the higher the mucilage content of soil, the more stable its aggregates (Wang et al. 2013b). Organic matter enhances the soil structure stability mainly by increasing soil cohesion and water repulsion (Chenu et al. 2000). Zhang et al. (1996) showed that the formation of water-stable aggregates in red soils depends mainly on the cementation of organic matter.  $Fe^{3+}$ ,  $Al^{3+}$  and kaolinite can jointly promote aggregation with organic matter (Six et al. 2000), while aluminum oxides and their hydrates can improve aggregate stability by synergizing with organic matter and mucilage (Molina

et al. 2001).

One of the key indicators in studying soil erosion resistance is the specific gravity and stability of water-stable aggregates with particle size  $>0.25$  mm (Bernard and Roose 2002; Cotler and Ortega 2006; Amézketa 1999). At present, most of the numerous studies on soil aggregates are based on simulated rainfall conditions. These studies include physical, chemical and biological indicators in soil, but there are few studies on the transport fragmentation characteristics of soil aggregates in concentrated water flow under different slope conditions (Karlen et al. 1992). Su et al. (2017) found that differences in both slope position and layout of plants affected the response of soil to runoff scour. A long-term observational experimental study (Tu et al. 2019) indicated that among the different land use patterns in red soil slopes studied, sediment loss and runoff were greatest in the farming area. Further studies were conducted on the soil of different land use patterns. For example, Shrestha and Lal (2008) studied the differences in the physical properties of soil in different land use patterns (forest, pasture and rangeland) in Ohio after 28 years of reclamation and found significant differences in the physical properties of the soil under different use patterns. McGrath et al. (2001) compared the differences in the soil pH, cation exchange, and soil nutrients in natural forest, rangelands, croplands, and plantations in the Amazon, and the results of their study indicated significant changes in the soil properties after land use changes. Zeng et al. (2018) showed that the aggregate stability of woodland soil under different rainfall conditions was higher than that of both grassland and forest grassland. In addition, Caravaca et al. (2004) found that the stability of woodland soil aggregates was significantly higher than that of arable soil. Red soil is a zonal soil in tropical and subtropical regions of China. The red soil developed from Sandshale is a representative soil of central subtropics. However, for the Sandshale red soil area with serious soil erosion, there are few studies on soil aggregates of different land use patterns.

The Sandshale red soil area is the main production area of grain, oil crops and fruits. Economic and social development and human population growth have intensified the pressure on the ecological environment and natural resources. Under the high-temperature and rainy conditions in southern China, the red soil and its parent material

are easily weathered and lost, resulting in infertile, sandy soil and serious soil erosion, which, together with the high land-use rate and re-cultivation index of the region, leads to differences in the soil erosion characteristics of the Sandshale red soil and those of other regions. The abundant local precipitation and improper land use have led to an accelerated rate of change in the soil properties, and human interference and damage reach far beyond the range of the capacity of the soil to self-regulate, resulting in very severe soil erosion (Reza et al. 2018). Among these interferences, land use patterns, as the most direct means of human interaction with natural processes, play a role in improving or hindering soil erosion. Land use patterns can change soil structure, organic cementing matter, and soil microbial activity. It causes recombination and redistribution of soil organic matter in the soil aggregates, which in turn affects the stability of the soil aggregates (Yang et al. 2003; Li et al. 2014; Yang et al. 2009). Many researchers have used land use patterns as an entry point to study the stability of soil aggregates. However, the Sandshale red soil area is currently understudied, with insufficient understanding and research in the area, and its research potential and comprehensive value have not been fully exploited. Thus, when water and soil conservation planning measures and soil erosion hazard assessments are carried out, a scientific and rational theoretical basis for these efforts is lacking, ultimately affecting planning and prevention efforts (Dlapa et al. 2011; Fattet et al. 2011). Hills and mountains are the main landforms in the Sandshale red soil area, and the complex geological environment has created diverse land use patterns such as arable land, orchard and woodland. *Pinus massoniana* and *Eucalyptus robusta* are typical plantation species in the region, with a wide plantation area and obvious ecological functions; they are gradually becoming the dominant species in the region. Therefore, soil from six typical land use patterns, namely natural forest, *Pinus massoniana*, *Eucalyptus urophylla* × *E. grandis*, wasteland, orchard and arable land, were selected for this study.

The objectives of this study were to (i) study the stability of soil aggregates and their mechanisms under six land use patterns in the Sandshale red soil area; (ii) study the transport and destruction patterns of soil aggregates under the action of concentrated water flow in different land use patterns and the influencing factors; and (iii) further clarify the

interrelationship between soil aggregate stability and soil erosion.

## 2 Materials and Methods

### 2.1 Study area

The Sandshale red soil area is located in the city of Liuzhou, Luzhai County, in the northeastern Guangxi Zhuang Autonomous Region of China (109°43'46"-109°58'18"E, 24°37'25"-24°52'11"N), with an east-west distance of 25 km and a north-south distance of 60 km. The geographical location of the study area is shown in Fig. 1. The sampling site is located at the foot of Tianping Mountain, with a river running through it and hilly terrain on both sides of the river; the relative elevation difference at the site is between 200 and 400 m, reaching 500 m in some areas, and the highest elevation is 895.9 m. The local area has a subtropical monsoon climate with high temperature and high humidity, and sufficient annual sunshine. The average annual temperature is approximately 19°C, the average annual rainfall is approximately 1760 mm, and the peak rainfall period is from April to August every year, with heavy and frequent rainfall and sufficient moisture. The study area receives abundant local rainfall, with synchronized changes in rain and temperature conditions, has a long frost-free period, and has a rainfall coefficient of 92.1, which indicates that the

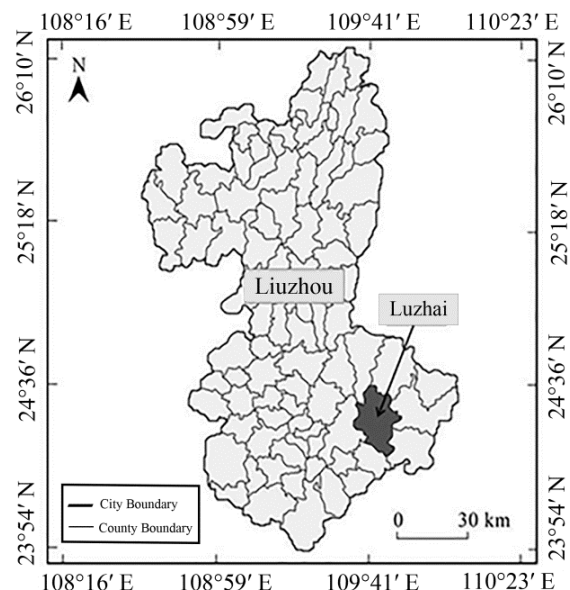


Fig. 1 Geographical location of the study area.

area contains sufficient moisture. Most of the local area has sandy shale and interbedded mudstone as the parent rock for soil formation, and red loam is widely distributed in the area, with a topsoil thickness range of 20-25 cm, a soil thickness range of approximately 50-70 cm, and a soil pH of approximately 5.8 (Zhang et al. 2008). The local forest is rich in resources, with various species of trees such as *Pinus massoniana*, *Eucalyptus urophylla* × *E. grandis*, *Cunninghamia lanceolata*, *Cinnamomum camphora* and *Schima superba* (Zhang et al. 2004). The study area not only includes farmland and orchard, but also has large areas of planted and natural woodland, with a diversity of land use patterns and is easy to sample.

The natural forest, *Pinus massoniana* and *Eucalyptus urophylla* × *E. grandis* sampling sites have good vegetation growth, a wide variety of understory vegetation and a high plant coverage degree on the ground surface. In the study area, the natural forest is an evergreen deciduous broadleaf mixed forest community. The dominant species in the tree layer is the *Schima superba*, followed by the evergreen or deciduous broadleaf species of *Triadica cochinchinensis*, *Liquidambar formosana* and *Mallotus paniculatus*; the dominant species in the shrub layer are *Heptapleurum heptaphyllum* and *Breynia fruticosa*, and the other species are mainly *Smilax arisanensis*, *Itea chinensis* and *Embelia laeta*; the dominant species in the herb layer is *Woodwardia japonica*, followed by *Lygodium flexuosum*, *Adiantum flabellulatum* and *Lophatherum gracile*. Natural forests are undisturbed and unmanaged. *Pinus massoniana* and *Eucalyptus urophylla* × *E. grandis* have artificial management measures such as fertilization in the early years and long-term management activities, such as the pruning every autumn and winter. They are subject to less human interference than orchard and cultivated land. The vegetation under woodland conditions mainly includes *Ficus esquiroliana*, *Pteris semipinnata*, *Clerodendrum cyrtophyllum*, *Bidens pilosa*, *Maesa japonica* and *Hypolepis punctata*. The orchards are mainly planted with citrus. Orchards are dominated by the growth of fruit trees and the ground is not well covered with plants due to human management. The main crop grown in the study area is *Zea mays*. Arable land due to long-term cultivation activities, and wasteland due to long-term land exposure, exhibit severe soil erosion.

## 2.2 Sample collection

The study area is dominated by hilly terrain, with most land use patterns on 10°-20° slopes; the studied soil belongs to the Ultisol. In this study, six different land use patterns were selected with slopes between 10° and 20°, similar slope direction and slope position, and red loam as the soil type: including natural forest (NF), *Pinus massoniana* (PM), *Eucalyptus urophylla* × *E. grandis* (EU), orchard (OR), wasteland (WL) and arable land (AL). Mature forestland was selected for sampling. Intact soil layers were selected for sampling, and six sample plots measuring 20 m × 20 m were randomly established within each of the six different land use patterns. To minimize errors arising from the experiment process, three sampling points were established in the sample plots in areas representative of land use characteristics. Before the collection of soil samples, the dead leaf layer on the soil surface was removed, and the sampling site was excavated at an appropriate distance from the base of tree trunks. The majority of the soil was present in the A layer, but more of the A layer had been eroded. Samples were taken from the surface layer of the soil down the profile, and samples were collected in 2 layers, with A layer and B layer of the soil selected according to the soil horizon. To collect samples for soil physical and chemical property analysis, the soil was collected from the 2 layers, A and B, in an “S” shape, and 3 replicates were collected in each layer. During the sampling process, undisturbed soil was collected using the cutting ring (100 cm<sup>3</sup>) and brought back to the laboratory for determination of soil physical properties, and another 30-40 kg of undisturbed soil samples were collected in rigid plastic boxes for soil aggregate analysis.

## 2.3 Measurement method

The basic soil physical and chemical properties were determined by conventional methods (Bao 2000). The soil bulk density was obtained by the cutting ring method; the soil textural composition was measured by the pipette method; the soil organic matter content was obtained by the potassium dichromate external heating method; the soil pH was determined using the 1:2.5 soil to water ratio potentiometric method; the cation exchange capacity (CEC) was measured by the CH<sub>3</sub>COONH<sub>4</sub> exchange method (Lin et al. 2022). Free iron and aluminum

(Fe<sub>a</sub> and Al<sub>a</sub>) were extracted using citrate-bicarbonate-dithionite (CBD) and ammonium oxalate (Wu et al. 2016), respectively, and the content of each was determined by inductively coupled plasma optical emission spectrometry (ICPS-7510, Shimadzu Corporation, Japan).

Aggregate stability was determined using the traditional wet sieving method (Sarkar 2005) and the Le Bissonais (LB) method (Le Bissonais 1996), which enabled the differentiation of soil aggregates into different damage mechanisms.

The concentrated water scouring experiment was conducted using a variable-slope flume with a specification size of 3.8 m × 0.2 m × 0.15 m, as shown in Fig. 2. Soil aggregates were used to simulate the soil surface roughness in the field, and soil aggregates scouring experiments were performed, which included 2 representative slopes (10° and 20°), aggregates from six land use patterns (OR, AL, WL, EU, PM and NF), 2 soil layers (A layer, B layer) and 5 transport distances (9 m, 18 m, 36 m, 54 m and 72 m) in 120 combinations, and each combination was replicated three times. Hydrodynamic parameters in the concentrated water flow were the water flow rate (10° slope: 0.47 m·s<sup>-1</sup>; 20° slope: 0.56 m·s<sup>-1</sup>), Reynolds number *Re* (10° slope: 1972; 20° slope: 2109), Darcy-Weisbach friction coefficient *f* (10° slope: 0.26; 20° slope: 0.35), flow shear stress  $\tau$  (10° slope: 7.26 Pa; 20° slope: 13.55 Pa) and stream power  $\omega$  (10° slope: 3.43 kg·m<sup>-3</sup>; 20° slope: 7.58 kg·m<sup>-3</sup>).

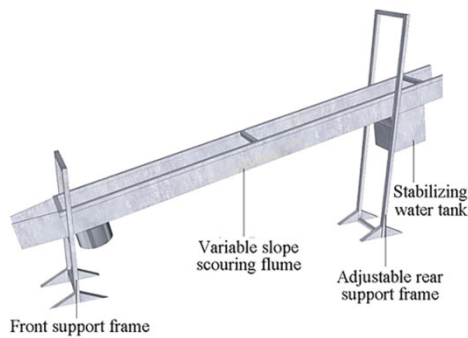


Fig. 2 Variable slope steel water flume.

## 2.4 Data calculation

### 2.4.1 Calculation of the index of soil properties

The mean weight diameter (MWD, mm) and >0.25 mm particle size water-stable aggregate content (WSA, %) are calculated as follows:

$$MWD = \sum_{i=1}^n X_i W_i \quad (1)$$

$$WSA_{0.25} = \frac{C_w}{C_t} \quad (2)$$

where,  $X_i$  denotes the average diameter of soil in each particle size range (mm);  $W_i$  denotes the proportion of soil aggregates at particle size  $i$  to the total number of aggregates;  $C_w$  represents the content of wet sieving aggregates >0.25 mm particle size;  $C_t$  represents the total number of aggregates.

The relative dissipation index (RSI) and relative mechanical crushing index (RMI) are calculated as follows (Le Bissonais 1996; Zhang and Horn 2001):

$$RSI = (MWD_{SW} - MWD_{FW}) / MWD_{SW} \times 100\% \quad (3)$$

$$RMI = (MWD_{SW} - MWD_{WS}) / MWD_{SW} \times 100\% \quad (4)$$

where,  $MWD_{FW}$ ,  $MWD_{SW}$ ,  $MWD_{WS}$  are the average weight diameter under fast wetting, slow wetting and wetting oscillation treatments, respectively.

Soil aggregate exfoliation fragmentation coefficient ( $\alpha$ ) is calculated as follows:

$$\alpha = \frac{\ln W_r / W_i}{x} \quad (5)$$

where,  $W_r$  and  $W_i$  denote the mass of aggregates that finally remain on the 0.25 mm soil sieving after transport  $x$ (m) versus the mass of aggregates before flushing, respectively.

### 2.4.2 Statistical analysis

Data statistics, analysis of variance (ANOVA) and correlation analysis were performed on the experiment results using Excel, SPSS 11.0 software. ANOVA was carried out using SPSS software to obtain the effect of different land use patterns on the extent of denudation damage to soil aggregates under concentrated water flow. The analysis of variance significance was carried out using the Duncan method at a significant level of  $P < 0.05$ . Trends in the relevant data were plotted using OriginPro 8.0 and Microsoft Excel 2010.

## 3 Results and Analysis

### 3.1 Basic physicochemical properties of red soil

The basic physicochemical properties of the six experiment soil are shown in Table 1. As shown in Table 1, soils from all six land use patterns exhibited acidity and low pH values, with little difference,

**Table 1** Analysis of basic physical and chemical properties of red soil under different land use patterns.

LUP	Sh	Shd (cm)	pH	Soil Organic Matter (g·kg <sup>-1</sup> )	Bulk Density (g·cm <sup>-3</sup> )	Total Porosity (%)	Capillary Porosity (%)	Non-capillary Porosity (%)	Cation Exchange Capacity (cmol·kg <sup>-1</sup> )	Fe <sub>d</sub> (g·kg <sup>-1</sup> )	Al <sub>d</sub> (g·kg <sup>-1</sup> )
NF	A	0-30	4.69±0.01c	29.94±0.98a	1.16±0.08e	56.51±2.95a	37.51±3.50a	19.01±0.55a	22.48±1.66a	15.68±0.53a	2.58±0.11a
	B	30-60	4.72±0.06bc	15.97±0.18de	1.29±0.05abcd	51.52±2.06bcde	40.73±1.52a	10.79±0.54de	13.57±0.64ef	12.25±1.41cd	2.05±0.09cd
WL	A	0-20	4.82±0.02ab	28.08±1.08cd	1.36±0.04bcde	48.68±1.37abcd	39.35±2.13a	9.40±0.76bcd	21.62±3.20ab	10.51±0.70def	1.99±0.05cde
	B	20-40	4.68±0.04c	15.21±0.25e	1.30±0.06abc	50.97±2.20cde	39.80±5.40a	11.17±3.20cde	13.32±1.68f	10.13±0.67ef	1.87±0.07ef
PM	A	0-25	4.54±0.01d	18.58±1.09b	1.23±0.03cde	53.76±1.13abc	39.88±1.52a	13.89±0.39bc	15.58±1.50def	13.16±1.02bc	2.22±0.05b
	B	25-50	4.68±0.04c	20.98±0.47g	1.36±0.03ab	48.91±1.14de	39.88±1.71a	9.03±0.57e	13.90±0.50ef	10.29±1.08ef	2.13±0.04bc
OR	A	0-25	4.89±0.01a	19.81±0.77bc	1.18±0.03de	55.73±1.21ab	41.41±1.03a	14.03±0.19b	17.39±1.33cd	8.78±0.31f	1.78±0.11f
	B	25-50	4.73±0.08bc	23.90±1.86ef	1.31±0.03abc	50.57±1.27cde	40.04±3.24a	10.53±1.97de	16.76±0.37cde	11.45±0.78cde	1.94±0.02de
EU	A	0-20	4.70±0.07bc	25.41±1.84e	1.30±0.04abc	50.91±1.67cde	39.66±2.86a	11.25±1.19cde	17.68±0.46cd	12.11±0.34cd	2.12±0.05bc
	B	20-40	4.71±0.06bc	31.98±0.49fg	1.39±0.06a	47.51±2.34e	38.21±2.53a	9.30±0.19e	17.80±0.80cd	14.78±0.78ab	2.21±0.06b
AL	A	0-20	4.93±0.04a	28.24±1.81cd	1.42±0.04cde	47.68±1.69abc	39.08±3.20a	7.60±1.51b	19.18±1.24bc	9.84±0.23ef	1.95±0.04de
	B	20-40	4.85±0.06a	20.69±1.03g	1.32±0.04abc	50.33±1.33cde	39.83±1.34a	10.50±0.01de	16.34±0.45cdef	10.11±0.33ef	2.00±0.04cde

**Notes:** LUP: land use patterns; Sh: Soil horizons; Shd: Soil horizons depth; NF: natural forest; PM: *Pinus massoniana*; EU: *Eucalyptus urophylla* × *E. grandis*; OR: orchard; WL: wasteland; AL: arable land; SOM: soil organic matter; BD: bulk density; TP: total porosity; CP: capillary porosity; NP: non-capillary porosity; CEC: cation exchange capacity; Fe<sub>d</sub>, Al<sub>d</sub> mean free oxides. The letters in the table represent the results of Duncan, and different letters in the same column represent the significant difference ( $P < 0.05$ ).

varying from 4.54 to 4.93. The organic matter content is a key indicator of the quality of the soil and is an essential part of soil research (Tian et al. 2003; Liu et al. 2019). The variation in organic matter in the six experiment soils ranged from 10.69 to 29.94 g·kg<sup>-1</sup>, among which the organic matter content of NF was relatively high and that of AL was low. Among the six experimented soils, the soil bulk density of the B layer in EU was the highest at 1.39 g·cm<sup>-3</sup>, and the second highest was measured in the B layer in PM at 1.36 g·cm<sup>-3</sup>. The distribution of the soil pore space showed that the total soil porosity was highest in NF and lowest in EU. Soil total porosity (TP), capillary porosity (CP), non-capillary porosity (NP), CEC, Fe<sub>d</sub> and Al<sub>d</sub> decreased with increasing soil depth in each stand, while soil bulk density exhibited the opposite pattern.

Soil physical composition not only affects the transformation and effectiveness of soil nutrients, but also indirectly influences nutrient availability by altering the soil aeration properties and hydrothermal processes and thus the soil quality and aggregate

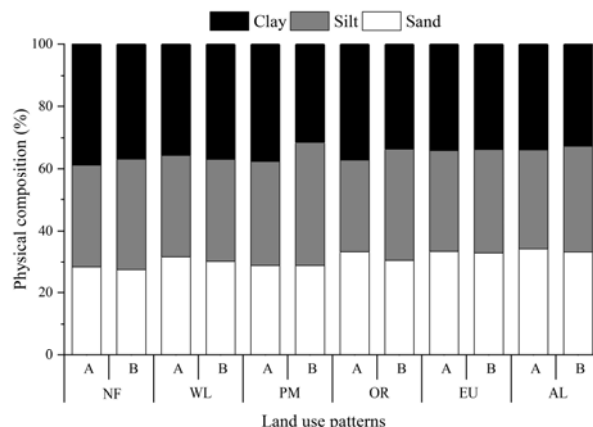


**Fig. 3** Physical composition of soil for six land use patterns. **Notes:** NF: natural forest; PM: *Pinus massoniana*; EU: *Eucalyptus urophylla* × *E. grandis*; OR: orchard; WL: wasteland; AL: arable land.

stability (Wang et al. 2016; Mamedov et al. 2007). The soil physical composition of the six land use patterns is shown in Fig. 3. Between different land use patterns, the clay content followed the order of NF>PM>OR>WL>EU>AL. NF had a higher clay

content than other land use and the lowest sand content; AL had a lower clay content than other land use patterns and the highest sand content. It could be concluded that NF had a well-developed plant root system, and its soil contained abundant mineral nutrients and had strong adhesion; the soil of AL was loose and had strong aeration and permeability, but weak adhesion. In terms of vertical variation, all six land use patterns exhibited a higher sand content in the A layer than in the B layer, which was generally consistent with the results of the above analysis of total soil porosity. This indicates that A layer has high sand content, high soil permeability, low cementation between soil particles, easy to be damaged by runoff and low soil impact resistance.

### 3.2 Stability characteristics of red soil aggregates

#### 3.2.1 Distribution characteristics of soil aggregates under the wet sieving treatment

Different land use patterns have a significant effect on the weight distribution of each particle size of soil aggregates, as has been shown previously (Ciric et al. 2012). The percent distribution of aggregates particle sizes measured by wet sieving is shown in Fig. 4, where aggregates with particle sizes of >2, 2-1, 1-0.5, 0.5-0.25, and <0.25 mm were present in the soil of all six land use patterns after wet sieving. With the exception of OR, the remaining five land use patterns were dominated by >2 mm aggregates, followed by 1-0.5 mm aggregates. Among the six experiment soils, the large aggregate content was relatively low in AL soil, and the percent distribution of microaggregates with a <0.25 mm particle sizes varied from 20% to 28%. In the A layer of the soil, the distribution of large aggregates with a >0.25 mm particle size for the six land use patterns ranked in the following order: NF>PM>WL>OR>EU>AL. In the B layer of the soil, the distribution of large aggregates with a >0.25 mm particle size ranked as follows: WL>NF>EU>OR>PM>AL. Although the distribution of large aggregates with >0.25 mm particle size was high in OR, most of the aggregates were concentrated in the 0.5-0.25 mm particle size, and the distribution of aggregates >2 mm in size accounted for a relatively low percentage. From this, it can be concluded that in the two soil layers, A and B, the distribution of large aggregates was higher in WL and NF and lower in OR and AL.

#### 3.2.2 Stability characteristics of soil aggregates under the wet sieving treatment

The soil mean weight diameter (MWD) was first proposed by Van Bavel (1950). The MWD value can indicate the average particle size and agglomeration degree of soil aggregates. The larger the MWD value is, the more stable the aggregate, and vice versa (Cerdeira 1998). With the use of the wet sieving method, the obtained indicators of soil aggregate stability under different land use patterns are shown in Table 2. The differences in MWD and WSA of water-stable soil aggregates were highly significant between the various land use patterns, with a distribution of NF>PM>WL>EU>AL>OR. The variation in the of MWD values for the six land use patterns under the

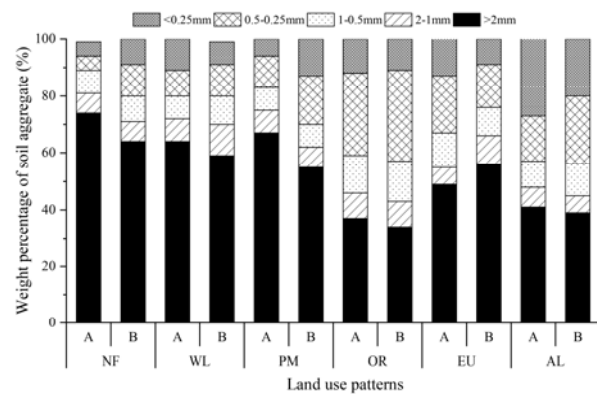


Fig. 4 Weight percentage of soil aggregates in different soil layers under different land use patterns.

Table 2 Aggregate stability of different land use patterns measured by the wet sieving method.

Land use patterns	Soil layer	MWD (mm)	WSA (%)
NF	A	4.81±0.36a	94.79±2.20a
	B	4.14±0.25ab	90.98±0.01ab
WL	A	4.25±0.96ab	89.45±6.52ab
	B	3.88±0.13abc	91.66±3.24ab
PM	A	4.37±0.60ab	94.22±0.41a
	B	3.74±0.81abcd	86.56±3.44ab
OR	A	2.50±0.82d	87.99±7.42ab
	B	2.45±0.62d	89.44±1.42ab
EU	A	3.29±0.20bcd	86.12±0.88ab
	B	3.68±0.09abcd	90.70±0.64ab
AL	A	2.77±0.43cd	72.30±12.61c
	B	2.72±0.04cd	79.85±3.90bc

Notes: NF: natural forest; PM: *Pinus massoniana*; EU: *Eucalyptus urophylla* × *E. grandis*; OR: orchard; WL: wasteland; AL: arable land; MWD: mean weight diameter; WSA: >0.25 mm particle size water-stable aggregate content. The letters in the table represent the results of Duncan, and different letters in the same column represent the significant difference ( $P<0.05$ ).

wet sieving method ranged from 2.45 to 4.81 mm, with NF having the largest MWD and OR having the smallest. The variation in the WSA values ranged from 72.30% to 94.79%, with the highest values in NF and the lowest values in AL, in general agreement with the distribution of >0.25 mm grain size. This indicates that after wet sieving treatment, the soil aggregate structure of NF is relatively stable and has a stronger resistance to soil erosion, while the aggregate structures of AL and OR are poorer and have a lower resistance to fragmentation. It was observed that different land use patterns significantly affected soil structural stability.

### 3.2.3 Stability characteristics of soil aggregates under the LB method treatment

The MWD values of the soil aggregates obtained by the LB method are shown in Table 3. Under the rapid wetting treatment, the MWD values for the different land use patterns were ranked in the following order: NF (1.18 mm) > PM (1.05 mm) > WL (0.91 mm) > OR (0.835 mm) > EU (0.82 mm) > AL (0.64 mm). Under the slow wetting treatment, the MWD values varied from 1.91 to 2.00 mm, with the largest in the A layer of NF and the smallest in the A layer of AL. Under the prewetting oscillation treatment, the MWD values varied from 1.56 to 2.00 mm, with the largest in the B layer of EU and the smallest in the A layer of AL. The MWD values were significantly different between the three different treatments, specifically  $MWD_{SW} > MWD_{WS} > MWD_{FW}$ , and this conclusion was consistent with the findings

of Li et al. (2005) and Yan et al. (2008). Among them, the  $MWD_{FW}$  values exhibited the largest difference, while the  $MWD_{SW}$  values exhibited the smallest difference.

The sensitivities of soil aggregates to different crushing mechanisms differed among the land use patterns. The relative dissipation index (RSI) and relative mechanical fragmentation index (RMI) were used to characterize the sensitivity of different soil aggregates to dissipation and external mechanical fragmentation (Ye et al. 2017; Zhang and Hom 2001). Aggregates with larger RSI and RMI values are more sensitive to dissipation and mechanical fragmentation, respectively. As shown in Table 3, among all the experiment soil, the RSI values ranked in the order of  $NF > WL > AL > PM > OR > EU$ . The variation in RMI values ranged from 0.23% to 3.56%, with the largest in the A layer of PM and the smallest in the A layer of EU. Overall, the RSI and RMI values showed significant differences under different land use patterns. Soil aggregates in NF showed a high sensitivity to dissipative effects, while soil aggregates in PM showed a high sensitivity to external mechanical destructive effects.

### 3.2.4 Relationship between the basic physical and chemical properties of aggregates and stability

The correlation analysis of basic soil properties and stability parameters are shown in Fig. 5. With the use of the wet sieving method, the sand content was significantly correlated with both MWD and WSA values. MWD values were negatively and significantly

**Table 3** Aggregate stability of different land use patterns and its related indexes measured by the LB method.

Land use patterns	Soil layer	MWD (mm)			RSI	RMI
		FW	SW	WS		
NF	A	1.53±0.01a	1.94±0.01e	1.99±0.01a	1.57±0.13ab	0.52±0.74cd
	B	0.82±0.02ef	1.97±0.01d	1.86±0.01cd	1.50±0.59ab	1.51±0.12bc
WL	A	0.93±0.01de	1.99±0.01bcd	1.83±0.05b	0.80±0.35a	0.62±0.04ab
	B	0.89±0.07de	1.98±0.01abc	1.90±0.02d	1.98±1.21abc	2.15±1.15bcd
PM	A	1.21±0.07bc	1.98±0.01abcd	1.96±0.01a	0.85±0.77abc	1.31±0.46bc
	B	0.88±0.04de	2.00±0.01a	1.84±0.04d	1.31±0.13abc	3.56±0.17a
OR	A	0.65±0.26fg	1.99±0.01ab	1.85±0.01d	0.56±0.57bc	0.64±1.73bcd
	B	1.02±0.07cde	2.00±0.01a	1.96±0.01a	0.87±0.10abc	0.54±0.20cd
EU	A	1.03±0.08cd	1.99±0.01abc	1.89±0.01bc	0.19±0.01c	0.23±0.07cd
	B	1.39±0.01ab	1.91±0.01f	2.00±0.01a	0.20±0.14c	0.40±0.11d
AL	A	0.61±0.01g	1.97±0.02d	1.49±0.01f	1.17±0.09abc	1.41±0.11bc
	B	0.66±0.02fg	1.98±0.01cd	1.56±0.02e	1.02±0.25abc	0.59±0.24bcd

**Notes:** NF: natural forest; PM: *Pinus massoniana*; EU: *Eucalyptus urophylla* × *E. grandis*; OR: orchard; WL: wasteland; AL: arable land; MWD: the mean weight diameter; FW: fast wetting; SW: slow wetting; WS: mechanical breakdown by shaking after pre-wetting; RSI: relative slaking index; RMI: relative mechanical breakdown index. The letters in the table represent the results of Duncan, and different letters in the same column represent the significant difference ( $P < 0.05$ ).



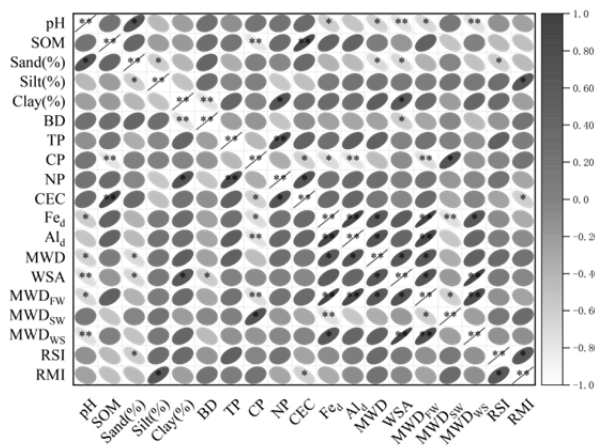


**Fig. 5** Correlation analysis of basic soil properties and stability parameters. **Notes:** SOM: soil organic matter; BD: bulk density; TP: total porosity; CP: capillary porosity; NP: non-capillary porosity; CEC: cation exchange capacity; Fe<sub>d</sub>, Al<sub>d</sub> mean free oxides; MWD: the mean weight diameter; WSA: the >0.25 mm particle size water-stable aggregate content; MWD<sub>FW</sub>: fast wetting; MWD<sub>SW</sub>: slow wetting; MWD<sub>WS</sub>: mechanical breakdown by shaking after pre-wetting; RSI: the relative slaking index; RMI: the relative mechanical breakdown index.

\* indicates a significant correlation ( $P < 0.05$ ), \*\* indicates a highly significant correlation ( $P < 0.01$ ).

correlated with sand content and positively correlated with Fe<sub>d</sub> and Al<sub>d</sub> content. The WSA values were significantly negatively correlated with sand content and soil capacity and positively correlated with clay content. In the LB method, the Fe<sub>d</sub> content was significantly and positively correlated with the MWD value except for the slow wetting treatment. Al<sub>d</sub> content was highly significantly and positively correlated with MWD<sub>FW</sub>, and CEC was significantly and negatively correlated with RMI values.

### 3.3 Transport characteristics of red soil aggregates under concentrated water flow

#### 3.3.1 Degree of aggregate exfoliation damage after different transport distances

The  $W_r/W_i$  value represents the ratio of the mass of >0.25 mm aggregates remaining to the mass of the original aggregates after flushing. The lower the  $W_r/W_i$  value is, the less >0.25 mm aggregates remain after scouring, representing a greater fragmentation of aggregates under a concentrated water flow. The  $W_r/W_i$  values for the soil from six different land use patterns washed at different transport distances on 10° and 20° slopes are shown in Fig. 6. The  $W_r/W_i$  values after different transport distances were significantly different, significantly decreasing with increasing

scouring distance. The maximum  $W_r/W_i$  value for the aggregates was 79% at a 20° slope and 91% at a 10° slope, and the  $W_r/W_i$  value at a 20° washout was significantly lower than that at 10°. For soil from different land use patterns, the  $W_r/W_i$  values after concentrated water flushing were significantly different. The  $W_r/W_i$  values of the six land use patterns showed a range of: NF>PM>EU>WL>OR>AL. In particular, after 72 m of flushing, the  $W_r/W_i$  values of NF were significantly higher than those of the other land use patterns. With vertical change in soil depth, the vast majority of soils showed higher  $W_r/W_i$  values for the A layer soil than for the B layer soil under the same land use pattern. However, after transport distances of 54 m and 72 m, the  $W_r/W_i$  values of the WL and AL soils were larger in the B layer than in the A layer.

The results of the multifactor analysis of the effects of land use, soil layer, slope and transport distance on  $W_r/W_i$  are shown in Table 4. Land use, soil layer, slope and transport distance all showed highly significant correlations for  $W_r/W_i$ . Transport distance, slope and the comprehensive effect of land use patterns and soil layers have significant influence on  $W_r/W_i$ . As shown in Fig. 6, it can be clearly seen that  $W_r/W_i$  gradually decreases as the transport distance increases.

#### 3.3.2 Morphological characteristics of soil aggregates in concentrated water flow

The morphological characteristics of soil aggregates in concentrated water flow are shown in Fig. 7. With increasing transport distance and slope, the projected area and circumference of the aggregates gradually decrease and the stability decreases. The morphology of the aggregates becomes rounded with wear, approaching a spherical shape.

#### 3.3.3 Relationship between the degree of aggregate abrasion and its own stability

The correlation of soil aggregate stability parameters with the  $W_r/W_i$  values and abrasion coefficient  $\alpha$  values are shown in Table 5. The soil aggregate stability parameters obtained by different methods showed different correlations with  $W_r/W_i$  values and  $\alpha$  values after five different transport distances. In particular, the aggregate exfoliation damage rate  $\alpha$  reached a significant correlation with the MWD<sub>FW</sub> measured by the LB method. In contrast, the MWD<sub>SW</sub> measured by the LB method did not reach a significant correlation with  $W_r/W_i$  values and

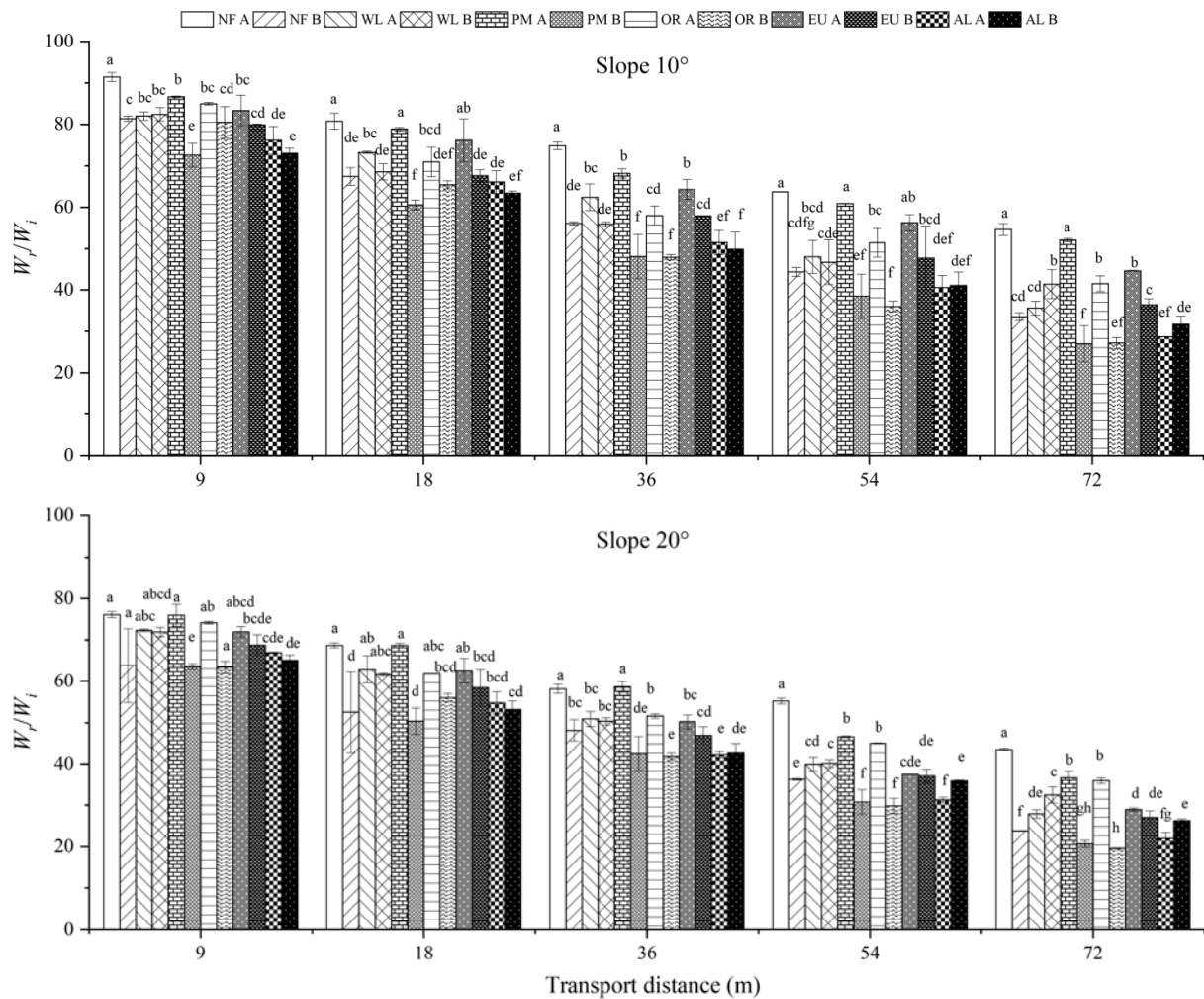


**Fig. 6** Comparison of  $W_r/W_i$  values of soil aggregates (the ratio between the residual weight and initial weight of soil aggregates) from the two soil horizons (A and B) after different transport distances for slopes at a)  $10^\circ$  and b)  $20^\circ$ . **Notes:** NF: natural forest; PM: *Pinus massoniana*; EU: *Eucalyptus urophylla* × *E. grandis*; OR: orchard; WL: wasteland; AL: arable land. The letters in the table represent the results of Duncan, and different letters in the same column represent significant differences at ( $P < 0.05$ ).

**Table 4** Interaction effect of land use patterns, soil layer, flume slope and transport distances on  $W_r/W_i$ .

Influencing factors	F	P
Land use patterns	135.333	< 0.001**
Soil layer	1091.450	< 0.001**
Flume slope	1588.964	< 0.001**
Transport distances	3555.513	< 0.001**
Land use patterns × Soil layer	161.881	< 0.001**
Land use patterns × Flume slope	10.074	< 0.001**
Land use patterns × Transport distances	3.054	0.008**
Soil layer × Flume slope	16.066	0.001**
Soil layer × Transport distances	4.206	0.012*
Flume slope × Transport distances	4.326	0.011*
Land use patterns × Soil layer × Transport distances	3.332	0.024*
Land use patterns × Soil layer × Transport distances	5.767	< 0.001**
Land use patterns × Flume slope × Transport distances	2.158	0.047*
Soil layer × Flume slope × Transport distances	3.356	0.030*

**Notes:** \* indicates a significant effect ( $P < 0.05$ ), \*\* means a highly significant effect ( $P < 0.01$ ).

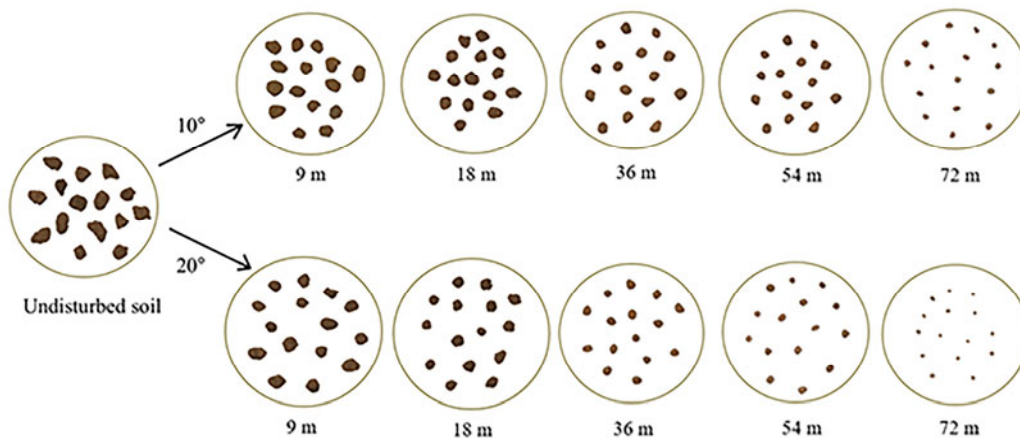


**Fig. 7** Morphological characteristics of soil aggregates in concentrated flow. The figure shows the morphological characteristics of soil aggregates under concentrated water scoured at different conditions. Fifteen representative aggregates were selected to be photographed.

**Table 5** Correlation of soil aggregate stability parameters with the  $W_r/W_i$  and abrasion coefficient  $\alpha$ .

Stability parameters		Wet sieving method		LB method			
		WSA	MWD	MWD <sub>FW</sub>	MWD <sub>SW</sub>	MWD <sub>WS</sub>	RMI
$W_r/W_i$	9 m	0.494	0.551	0.551	-0.213	0.459	-0.310
	18 m	0.534	0.569	0.562	-0.232	0.461	-0.344
	36 m	0.544	0.621*	0.564	-0.303	0.491	-0.350
	54 m	0.601	0.573	0.576	-0.320	0.539	-0.411
	72 m	0.697*	0.662*	0.632*	-0.343	0.560	-0.456
$\alpha$	9 m	-0.490	-0.502	-0.562*	0.214	-0.437	0.302
	18 m	-0.497	-0.511	-0.574**	0.243	-0.451	0.370
	36 m	-0.684**	-0.562*	-0.574**	0.308	-0.452	0.411
	54 m	-0.680**	-0.583**	-0.593**	0.331	-0.460	0.486*
	72 m	-0.702**	-0.581**	-0.641**	0.390	-0.653**	0.502*

**Notes:**  $W_r/W_i$ : the ratio between the residual weight and initial weight of soil aggregates;  $\alpha$ : abrasion coefficient; WSA: the >0.25 mm particle size water-stable aggregate content; MWD: the mean weight diameter; RMI: the relative mechanical breakdown index. FW, SW and WS mean fast wetting, slow wetting and mechanical breakdown by shaking after pre-wetting, respectively. \* indicates a significant effect ( $P < 0.05$ ), \*\* indicates a highly significant effect ( $P < 0.01$ ).

spalling damage coefficient  $\alpha$  values at all transport distances, and the correlation coefficient values were low, showing a low correlation with  $W_r/W_i$  and  $\alpha$ . In addition, the RMI measured by the LB method showed a negative correlation with  $W_r/W_i$  and a positive correlation with the value of the exfoliation coefficient  $\alpha$ . This indicates that the larger the value of RMI is, the larger the value of  $\alpha$ , the smaller the value of  $W_r/W_i$ , and the greater the fragmentation of the soil aggregates.

### 3.3.4 Particle size distribution of aggregates after exfoliation and destruction

After experiencing denudation damage under concentrated water flow with different transport distances, the soil aggregates of different land use patterns showed different results. In this experiment, the MWD (mm) of aggregates >0.25 mm was used to reflect the denudation damage effect of soil aggregates,

and the results are shown in Table 6. The MWD of >0.25 mm aggregates remaining after flushing gradually decreased with increasing transport distance, and the difference was very significant after a transport distance of 72 m. Under different slope conditions, the MWD of >0.25 mm aggregates obtained by scouring was greater on 20° slopes than on 10° slopes. This result indicated that the aggregates became severely fragmented with increasing slope. The MWD of the aggregates >0.25 mm after flushing were ranked in the order of NF>PM>EU>WL>OR>AL, with the same results as the above comparison of  $W_r/W_i$  values after different transport distances. Among them, the MWD value of NF reached 3.59 mm, while the value of AL under the same conditions was only 1.75 mm, which was less than half that of NF. With increasing depth in the soil profile, the MWD values of the aggregates >0.25 mm after different transport distances all showed a lower

value in the B layer of soil than in the A layer of soil. Most notably, the B layer significantly differed from the A layer after the transport distance increased to 54 m and 72 m.

The sensitivity of soil aggregates to external mechanical fragmentation has an important influence on their exfoliation damage results after scouring. The correlation between the mean weight diameter (MWD) and the relative mechanical fragmentation index (RMI) of aggregates >0.25 mm after different transport distances is shown in Table 7. The MWD values in the table were significantly correlated with the RMI values and all showed negative correlations.

The particle size distribution of soil aggregates >0.25 mm after different transport distances for the six land use patterns is shown in Fig. 8. The aggregate content of 5-2 mm, 2-1 mm, 1-0.5

mm, and 0.5-0.25 mm increased with the increase of transport distance, except for the aggregate content of >5 mm, which decreased with the increase of transport distance. It can be seen that in the same experiment soil and transport distance, the content of large-size aggregates with particle size >5 mm in the B layer is lower than that in the A layer, and decreases rapidly with increasing transport distance. It shows that under the same scouring conditions, the decomposition of large-size aggregates in the B layer soil occurs at a faster rate.

#### 4 Discussions

Land use patterns are the most direct human activity that affect soil (Meng et al. 2010; Tang et al.

**Table 6** Average weight diameter (MWD, mm) of aggregates > 0.25 mm after different transport distances.

Flume slope	Land use patterns	Soil layer	9 m	18 m	36 m	54 m	72 m
10°	NF	A	4.70±0.02a	4.56±0.05a	4.14±0.13a	4.03±0.06a	3.59±0.03a
		B	4.39±0.01cde	4.11±0.04e	3.97±0.11abc	3.55±0.02b	3.34±0.05bc
	WL	A	4.51±0.01b	4.43±0.0ab	3.82±0.09bcd	3.59±0.04b	3.50±0.04ab
		B	4.41±0.01cde	4.31±0.10bc	4.03±0.06ab	3.44±0.04b	2.98±0.04e
	PM	A	4.69±0.01a	4.50±0.05a	4.05±0.01ab	3.61±0.05b	3.36±0.01bc
		B	4.43±0.05cd	4.06±0.01e	3.24±0.16e	2.50±0.27d	2.21±0.06g
	OR	A	4.55±0.03b	4.33±0.12b	4.05±0.06ab	3.57±0.01b	3.28±0.07cd
		B	4.36±0.01e	4.30±0.06bcd	3.75±0.06cd	3.38±0.02b	3.08±0.03e
	EU	A	4.64±0.06a	4.30±0.01bcd	3.76±0.11cd	3.63±0.02b	3.13±0.02de
		B	4.37±0.02de	3.91±0.01f	3.60±0.12d	2.93±0.27c	2.77±0.06f
	AL	A	4.45±0.01c	4.16±0.06de	3.83±0.15bcd	3.55±0.01b	2.69±0.06f
		B	4.35±0.02e	4.19±0.05cde	3.37±0.04e	2.47±0.02d	1.75±0.24h
20°	NF	A	4.53±0.01a	4.42±0.01a	4.05±0.01a	3.66±0.06a	3.31±0.03a
		B	4.24±0.23d	3.85±0.31f	3.69±0.05c	3.47±0.04cd	2.88±0.03c
	WL	A	4.46±0.04ab	4.15±0.02bcde	3.90±0.08b	3.41±0.01d	3.04±0.12b
		B	4.40±0.09abcd	4.17±0.01bcd	3.89±0.02b	3.51±0.01bcd	3.09±0.08b
	PM	A	4.42±0.01abcd	4.36±0.03ab	3.99±0.02ab	3.57±0.01abc	3.16±0.04b
		B	4.27±0.05cd	3.92±0.01ef	3.37±0.09e	2.68±0.05g	2.49±0.03e
	OR	A	4.46±0.01abc	4.27±0.06abc	3.92±0.03b	3.62±0.01ab	3.09±0.01b
		B	4.34±0.05abcd	3.98±0.04def	3.61±0.01cd	2.87±0.14f	2.31±0.01f
	EU	A	4.37±0.05abcd	4.15±0.04bcd	3.65±0.02c	3.47±0.06cd	3.11±0.08b
		B	4.29±0.03bcd	4.14±0.01bcde	3.61±0.07cd	2.99±0.10f	2.71±0.03d
	AL	A	4.39±0.01abcd	4.04±0.01def	3.52±0.01d	2.95±0.02f	2.39±0.10ef
		B	4.32±0.01bcd	4.11±0.04cde	3.64±0.06cd	3.20±0.04e	2.33±0.01f

**Notes:** NF: natural forest; PM: *Pinus massoniana*; EU: *Eucalyptus urophylla* × *E. grandis*; OR: orchard; WL: wasteland; AL: arable land. The letters in the table represent the results of Duncan, and different letters in the same column represent significant differences at  $P<0.05$ .

**Table 7** Correlation coefficient between the average weight diameter (MWD) and the relative mechanical crushing index (RMI) of > 0.25 mm aggregates after different transport distances.

Stability parameters	Flume slope	RMI				
		9 m	18 m	36 m	54 m	72 m
MWD	10°	-0.245	-0.301	-0.302	-0.404	-0.338
	20°	-0.430*	-0.426*	-0.392	-0.394	-0.196

**Notes:** MWD: mean weight diameter. RMI: relative mechanical breakdown index. \* indicates a significant effect ( $P<0.05$ ).

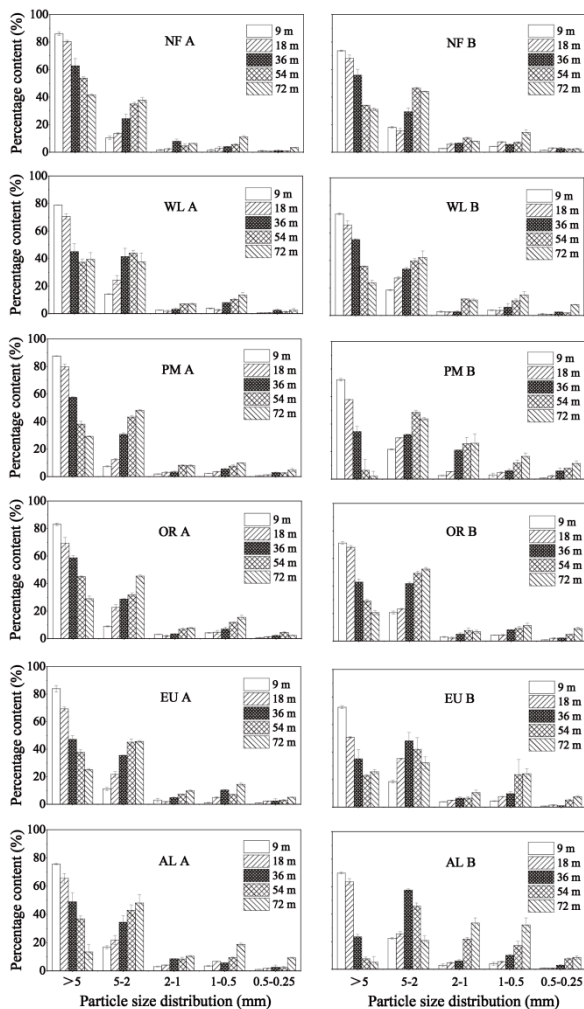


**Fig. 8** Particle size distribution of >0.25 mm aggregates after different transport distances. A and B are soil layers collected according to the soil horizon.

2015). To some extent, differences in land use patterns can cause changes in the physicochemical properties of soil, which in turn affect the soil quality and alter the stability of soil aggregates (Xu et al. 2007; Wei and Bin 2002; Kalhor et al. 2017). In this study, samples from different land use patterns in the Sandshale red soil area of Asia were used to analyze the particle size combination and stability of aggregates by combining the wet sieving method and the LB method, and the transport damage mechanism of aggregates was determined by a concentrated water scouring experiment.

Differences in the microenvironment of the soil occur under different land use patterns, leading to changes in the particle size distribution and stability of the water-stable soil aggregates (Liu et al. 2008; Zhang et al. 2008). This is similar to the findings of

Chen et al. (2012). Different land use patterns significantly affected the distribution and mean weight diameter (MWD) of aggregates. The highest distribution of large aggregates were measured in NF and the lowest in OR and AL. The clay grain contents were greater than 30% for all six land use patterns. According to the three-level classification of the international system of soil texture, the experiment soils all belonged to the clay soil class. Clay has high total porosity, rich in mineral nutrients, high number of colloids in the soil, strong adsorption capacity, dense structure, excellent water and fertilizer retention properties.

The stability of the water-stable aggregates was measured and showed a high stability in NF and a low stability in OR and AL, which was consistent with the results of Xiao and Shu (2021). Through the correlation analysis between the basic properties of soil and the stability parameters, the contents of  $Fe_d$  and  $Al_d$  show a strong correlation with the stability parameters. Numerous studies have shown that the cementation of aggregates is related to the contents of Fe and Al oxides (Zhang and Horn 2001; Onweremadu et al. 2007; Wagner et al. 2010; Li et al. 2010; Dela et al. 2021). Fe and Al oxides have a large surface area and are bound to soil clay particles by Coulombic forces, thus forming stable aggregates. Soil organic matter,  $Al_d$ ,  $Fe_d$ , and clay content are strongly correlated to soil aggregate stability. Microaggregates can continuously polymerize to form large aggregates under the cementing effect of organic matter, which makes the soil aggregates more stable.

In this study,  $W_r/W_i$  values were obtained by concentrated water scouring experiment. The results show that the  $W_r/W_i$  values under  $20^\circ$  scouring conditions were significantly lower than those at  $10^\circ$  slopes. This indicates that the slope has an important effect on the degree of denudation and destruction of aggregates during the scouring process. The degree of fragmentation of the soil aggregates gradually increased as the slope increased. The  $W_r/W_i$  values for the six land use patterns were ranked in the following order:  $NF > PM > EU > WL > OR > AL$ . With increasing depth in the soil profile, the  $W_r/W_i$  value of the A layer was greater than that of the B layer. We conducted a multifactorial analysis of the effects of land use, soil layer, slope and transport distance on  $W_r/W_i$ . The results again demonstrate that land use, soil layer, slope and transport distance all show highly significant correlations for  $W_r/W_i$ . In particular, the

transport distance and slope have significant effects on  $W_r/W_i$ .  $W_r/W_i$  has significant differences under the combination of land use patterns and soil layers. However, after transport distances of 54 m and 72 m, the  $W_r/W_i$  values of WL and AL were greater at the B layer than at the A layer. This indicates that NF, PM, EU and OR all have a stable surface soil structure. This is consistent with the findings of Liu et al. (2013), who concluded that the root system of trees played a strong role in soil consolidation and water retention, resulting in greater stability of the surface aggregates under the action of concentrated water flow in forests. Wasteland (WL) had a low vegetation cover, lacked management and care, and the cultivated land (AL) was frequently reclaimed and severely disturbed by humans. Cultivation led to a loose soil surface structure in arable land (AL) and orchard (OR), which were severely fragmented by water runoff.

By analyzing the denudation effect of concentrated water flow on soil aggregates, it was found that the projected area and perimeter of the aggregates gradually decrease with the increase of transport distance and slope, and the stability decreases. The movement pattern of soil aggregates in concentrated water flow is constantly changing. In the early stage of transportation, aggregates with larger particle size are mainly transported in a rolling mode (Wang et al. 2022). The aggregates with smaller particle size mainly show jumping and suspension transport mode. Then the MWD of  $>0.25$  mm aggregates was calculated and analyzed regularly. The conclusions are generally consistent with the results of  $W_r/W_i$  analysis. Correlation analysis of the MWD and RMI of  $>0.25$  mm aggregates showed that the RMI was negatively correlated with the MWD, which was consistent with the findings of Wang et al. (2011). This indicated that as the mechanical fragmentation susceptibility of the soil aggregates increased, the MWD of aggregates  $>0.25$  mm decreased after flushing and the degree of fragmentation was high.

The results showed that the stability of the soil aggregates differed significantly among the soil of the six land use patterns in the Sandshale red soil area. Changes in land use patterns may alter the amount of dead sediment and plant roots, the input of organic matter, and the percentage of the large aggregate content in the soil, which was consistent with the findings of Singh and Ghoshal (2014). The stability of the soil aggregates was high under three land use patterns, namely NF, PM and EU. This result

indicated that under woodland conditions, the vegetation cover was high, and compared to the frequently-managed AL and OR sites, the woodland growth process was less disturbed by humans and may also have been influenced by root secretions, which enhanced the soil stability. Therefore, the aggregates were more resistant to erosion in the woodland environment, which was consistent with the findings of Liu et al. (2015). The plant diversity of the experiment wasteland was increased when the land was rehabilitated by abandonment after many years. The surface layer of the soil receives fresh plant and animal residues directly, resulting in the formation of nutrients such as soil organic matter, which allows for better growth of soil microorganisms. This promotes the conversion of microaggregates to more cohesive large particle size aggregates or intermediate aggregates, resulting in improved soil structure (Demenois et al. 2018). However, due to the lack of management and care, the vegetation is unevenly distributed and has low cover, and is less resistant to erosion. The stability of soil aggregates in wasteland is lower than that in forest land (Zheng et al. 2009; Yang et al. 2003; Li et al. 2014). In comparison, the soil aggregates of AL and OR were less stable and had a weaker resistance to erosion. This indicates that AL and OR are under anthropogenic management, with a high frequency and intensity of use, and have a low ground cover, resulting in loose surface soil, dense soil pores, and a low specific gravity of large aggregates, which are prone to fragmentation under the action of external forces (Emadi et al. 2009; Bernard and Roose 2002; Amézketa 1999).

Overall, among the soil of the six land use patterns in the Sandshale red soil area, NF had the highest soil aggregate stability, a high soil quality, and a high erosion resistance. Conversely, the soil aggregates of AL had the lowest stability, a reduced soil quality and a low erosion resistance under high frequency disturbance, which was consistent with the findings of Dong (2011). It is thus clear that differences in land use patterns have a critical impact on the stability of soil aggregates. Improving the stability of soil aggregates plays a key role in enhancing soil productivity and minimizing soil erosion and degradation. Among the six land use patterns, the soil aggregates in the three types of forested environments were highly resistant to erosion. This indicated that for areas with serious soil erosion, strengthening forest construction while implementing natural forest

protection projects can not only reduce soil erosion and alleviate water pollution but also effectively enhance the soil quality and improve soil fertility so that the level of sustainable development can be improved. Therefore, the protection of agricultural land should be enhanced and the development of high-quality forests should be promoted. The results of the study may provide a scientific basis for maintaining high levels of land quality.

## 5 Conclusions

The stability of soil aggregates under different land use patterns in the Sandshale red soil area showed was ranked as follows: NF>PM>EU>WL>OR>AL. The stability of soil aggregates decreases decreased with increasing depth of the soil horizon. Arable land soils are were loose, disintegrating and have had low aggregate stability. Natural forest soils are were dense, and have had a high bulk density, a stable soil structure and the highest degree of aggregate stability. This indicates that the woodland environment plays an important role in maintaining a higher stability of soil aggregates and minimizing soil erosion and degradation phenomena. In this regard, it is important to pay attention to the current problems of insufficient total forest resources and low soil quality of arable soiland. Therefore, strengthening the construction of plantation forests and improving farming methods can be an effective measure for soil improvement in red soil hilly region, which is of great significance for the optimization of land-use structure as well as soil erosion control in red soil hilly region.

## Acknowledgments

We thank the financial support for the research provided by the National Natural Science Foundation

## References

- Abrahams AD, Parsons AJ, Luk SH (1986) Field measurement of the velocity of overland flow using dye tracing. *Earth Surf Process Landf* 11(6): 653-657.  
<https://doi.org/10.1002/esp.3290110608>
- Amézketa E (1999) Soil Aggregate Stability: A Review. *J Sustain Agric* 14(2): 83-151.  
[https://doi.org/10.1300/J064v14n02\\_08](https://doi.org/10.1300/J064v14n02_08)
- An SS, Darboux F, Cheng M (2013) Revegetation as an efficient means of increasing soil aggregate stability on the Loess Plateau (China). *Geoderma* 209: 75-85.  
<https://doi.org/10.1016/j.geoderma.2013.05.020>
- Bao SD (2000) *Soil and Agricultural Chemistry Analysis*. China

of China (No. 42107350), the Special Projects of the Central Government Guiding Local Science and Technology Development in China (Guike. ZY21195022) and the National Natural Science Foundation of China (No. 42007055). We thanked LENG Nuan, LIU Zhi-fei, SU Zi-mei and WEI Li-tian for their contributions during the experiments.

## Author Contribution

Wen Li-li: Investigation, Methodology, Data curation, Resources, Formal analysis, Software, Visualization, Writing-original draft, Writing-review & editing. Wang Jin-yue: Conceptualization, Visualization, Investigation, Supervision, Software. Deng Yu-song: Conceptualization, Methodology, Data curation, Supervision, Validation, Writing-review & editing. Duan Xiao-qian: Data curation, Funding acquisition, Writing-review & editing, Visualization, Supervision.

## Ethics Declaration

**Availability of Data/Materials:** The datasets generated during this study are available from the corresponding author upon reasonable request and within the framework of cooperation agreements and scientific research projects.

**Conflict of Interest:** No conflict of interest exists in the submission of this manuscript, and manuscript is approved by all authors for publication. I would like to declare on behalf of my co-authors that the work described is our original research that has not been published previously, nor under consideration for publication elsewhere, in whole or in part. All the authors listed have approved the submission of the manuscript enclosed.

- Agriculture Press, Beijing. (In Chinese)
- Bavel C (1950) Mean Weight-Diameter of Soil Aggregates as a Statistical Index of Aggregation. *Soil Sci Soc Am J* 14(C): 20-23.  
<https://doi.org/10.2136/sssaj1950.036159950014000C0005x>
- Bernard B, Roose E (2002) Aggregate stability as an indicator of soil susceptibility to runoff and erosion: Validation at several levels. *Catena* 47: 133-149.  
[https://doi.org/10.1016/S0341-8162\(01\)00180-1](https://doi.org/10.1016/S0341-8162(01)00180-1)
- Benavides IF, Solarte ME, Pabón V, et al. (2018) The variation of infiltration rates and physical-chemical soil properties across a land cover and land use gradient in a Paramo of southwestern Colombia. *J Soil Water Conserv* 73(4): 400-410.

- <https://doi.org/10.2489/jswc.73.4.400>
- Caravaca F, Lax A, Albaladejo J (2004) Aggregate stability and carbon characteristics of particle-size fractions in cultivated and forest soils of semiarid Spain. *Soil Tillage Res* 78: 83-90. <https://doi.org/10.1016/j.still.2004.02.010>
- Cerda A (1998) Soil aggregate stability under different Mediterranean vegetation types. *Catena* 32(2): 73-86. [https://doi.org/10.1016/S0341-8162\(98\)00041-1](https://doi.org/10.1016/S0341-8162(98)00041-1)
- Chen S, Yang F, Lin S, et al. (2012) Impact of land use patterns on stability of soil aggregates in red soil region of south China. *J Soil Water Conserv* 26: 211-216.
- Chenu C, Le Bissonnais Y, Arrouays D (2000) Organic matter influence on clay wettability and soil aggregate stability. *Soil Sci Soc Am J* 64(4): 1479-1486. <https://doi.org/10.2136/sssaj2000.6441479x>
- Ćirić V, Manojlović M, Nesić L, et al. (2012) Soil dry aggregate size distribution: effects of soil type and land use. *J Soil Sci Plant Nutr* 12(4): 689-703. <https://doi.org/10.4067/S0718-95162012005000025>
- Cotler H, Ortega-Larrocea MP (2006) Effects of land use on soil erosion in a tropical dry forest ecosystem, Cham-la watershed Mexico. *Catena* 65: 107-117. <https://doi.org/10.1016/j.catena.2005.11.004>
- Curtin D, Steppuhn H, Selles F (1994) Clay dispersion in relation to sodicity, electrolyte concentration, and mechanical effects. *Soil Sci Soc Am J* 58(3): 955-962. <https://doi.org/10.2136/sssaj1994.03615995005800030045x>
- Dela D, Kisi I, Bogunovi I, et al. (2021) Temporal impacts of pile burning on vegetation regrowth and soil properties in a Mediterranean environment (Croatia). *Sci Total Environ* 149318. <https://doi.org/10.1016/j.scitotenv.2021.149318>
- Demenois J, Carriconde F, Bonaventure P, et al. (2018) Impact of plant root functional traits and associated mycorrhizas on the aggregate stability of a tropical ferralsol. *Geoderma* 312: 6-16. <https://doi.org/10.1016/j.geoderma.2017.09.033>
- Dexter AR (1991) Amelioration of soil by natural processes. *Soil Tillage Res* 20: 87-100. [https://doi.org/10.1016/0167-1987\(91\)90127-J](https://doi.org/10.1016/0167-1987(91)90127-J)
- Dlapa P, Chrenková K, Hrabovský A, et al. (2011) The effect of land use on soil aggregate stability in the viticulture district of Modra (SW Slovakia). *Ekológia (Bratislava)* 30(4): 397-404. <https://doi.org/10.4149/ekol-2011-04-397>
- Dong LL (2011) Characteristics of soil water stable aggregates under different land-use types. *Linye Kexue* 47(4): 95-100. (In Chinese) <https://doi.org/10.3724/SP.J.1011.2011.00338>
- Emadi M, Baghernejad M, Memarian HR (2009) Effect of land-use change on soil fertility characteristics within water-stable aggregates of two cultivated soils in northern Iran. *Land Use Policy* 26(2): 452-457. <https://doi.org/10.1016/j.landusepol.2008.06.001>
- Ewing LK, Mitchell JK (1986) Overland flow and sediment transport simulation on small plots. *Trans ASAE* 29(6): 1572-1581. <https://doi.org/10.13031/2013.30356>
- Fattet M, Fu Y, Ghestem M, et al. (2011) Effects of vegetation type on soil resistance to erosion: Relationship between aggregate stability and shear strength. *Catena* 87(1): 60-69. <https://doi.org/10.1016/j.catena.2011.05.006>
- Jastrow JD, Miller RM (1996) Soil aggregate stabilization and carbon sequestration: feedbacks through organomineral associations. Argonne National Lab IL (United States). <https://doi.org/10.1201/9780203739273-15>
- Jastrow JD (1996) Soil aggregate formation and the accrual of particulate and mineral-associated organic matter. *Soil Biol Biochem* 28(4-5): 665-676. [https://doi.org/10.1016/0038-0717\(95\)00159-x](https://doi.org/10.1016/0038-0717(95)00159-x)
- Kalhor SA, Xu X, Chen W, et al. (2017) Effects of different land-use systems on soil aggregates: a case study of the Loess Plateau (Northern China). *Sustainability* 9(8): 1349. <https://doi.org/10.3390/su9081349>
- Karlen DL, Eash NS, Unger PW (1992) Soil and crop management effects on soil quality indicators. *Am J Alternative Agr* 7(1-2): 48-55. <https://doi.org/10.1017/S0889189300004458>
- Le Bissonnais Y (1996) Aggregate stability and assessment of soil crustability and erodibility: I. Theory and methodology. *Eur J Soil Sci* 47(4): 425-437. <https://doi.org/10.1111/j.1365-2389.1996.tb01843.x>
- Li H, Wang CY, Wen FT, et al. (2010) Distribution of organic matter in aggregates of eroded Ultisols, Central China. *Soil Tillage Res* 108(1-2): 59-67. <https://doi.org/10.1016/j.geoderma.2004.03.005>
- Li JL, Jiang CS, Hao QJ (2014) Impact of land use type on stability and organic carbon of soil aggregates in Jinyun mountain. *Environmental Science* 35(12): 4695-4704. (In Chinese) <https://doi.org/10.13227/j.hjkk.2014.12.037>
- Lin LW, Deng YS, Yang GR, et al. (2022) Using Le Bissonnais method to study the stability of soil aggregates in plantations and its influence mechanism. *Arch Agron Soil Sci* 68(2): 209-225. <https://doi.org/10.1080/03650340.2020.1829598>
- Liu L, Wang HY, Dai W (2019) Characteristics of soil organic carbon mineralization and influence factor analysis of natural Larix olgensis forest at different ages. *J For Res* 30(4): 1495-1506. <https://doi.org/10.1007/s11676-018-0724-4>
- Liu L, AN SS, Huang HW (2013) Application of le bissonnais method to study soil aggregate stability under different vegetation on the loess plateau. *Acta Ecologica Sinica* 33(20): 6670-6680. (In Chinese) <https://doi.org/10.5846/stxb201301160103>
- Liu XL, He YQ, Li CL, et al. (2008) Distribution and physical properties of soil water-stable aggregates in red soils in different land use and soil fertility. *Acta Pedologica Sinica* 45(3): 459-465. (In Chinese) <https://doi.org/10.3321/j.issn:0564-3929.2008.03.011>
- Liu Y, Chengliang LI, Gao M, et al. (2015) Effect of different land-use patterns on physical characteristics of the soil in the Yellow River delta region. *Acta Ecologica Sinica* 35(15): 5183-5190. (In Chinese) <https://doi.org/10.5846/stxb201312253030>
- Li ZX, Cai CF, Shi ZH, et al. (2005) Aggregate Stability and Its Relationship with Some Chemical Properties of Red Soils in Subtropical China. *Pedosphere* 15(001): 129-136. <https://doi.org/10.1007/s10705-004-5083-1>
- Lu J, Zheng FL, An J (2016) An experimental study of Mollisol aggregate loss characteristics during rainfall erosion processes. *Acta Ecologica Sinica* 36(8). (In Chinese) <https://doi.org/10.5846/stxb201410282108>
- Mamedov AI, Beckmann S, Huang C, et al. (2007) Aggregate stability as affected by polyacrylamide molecular weight, soil texture, and water quality. *Soil Sci Soc Am J* 71(6): 1909-1918. <https://doi.org/10.2136/sssaj2007.0096>
- McGrath DA, Smith CK, Gholz HL, et al. (2001) Effects of land-use change on soil nutrient dynamics in amazônia. *Ecosystems* 4(7): 625-645. <https://doi.org/10.1007/s10021-001-0033-0>
- Meng QH, Fu BJ, Yang LZ (2010) Effects of land use on soil erosion and nutrient loss in the Three Gorges Reservoir Area, China. *Soil Use Manage* 17(4): 288-291. <https://doi.org/10.1111/j.1475-2743.2001.tb00040.x>
- Molina NC, Caceres MR, Pietrobomi AM (2001) Factors affecting aggregate stability and water dispersible clay of recently cultivated semiarid soils of Argentina. *Arid Land Res Manag* 15(1): 77-87. <https://doi.org/10.1080/15324980118369>
- Onweremadu EU, Onyia VN, Anikwe MAN (2007) Carbon and nitrogen distribution in water-stable aggregates under two tillage techniques in fluvisols of Owerri area, southeastern Nigeria. *Soil Tillage Res* 97(2): 195-206. <https://doi.org/10.1016/j.still.2007.09.011>
- Opara CC (2009) Soil microaggregates stability under different land use types in south eastern Nigeria. *Catena* 79(2): 103-112. <https://doi.org/10.1016/j.catena.2009.06.001>
- Reza SK, Baruah U, Nayak DC, et al. (2018) Effects of land-use on soil physical, chemical and microbial properties in humid subtropical Northeastern India. *Natl Acad Sci Lett* 41(3): 141-145. <https://doi.org/10.1007/s40009-018-0634-1>
- Sarkar D (2005) Physical and chemical methods in soil analysis.



- New Age International.
- Shi FS, Wang JN, Lu T, et al. (2013) Effects of different types of vegetation recovery on runoff and soil erosion on a Wenchuan earthquake-triggered landslide, China. *J Soil Water Conserv* 68(2): 138-145. <https://doi.org/10.2489/jswc.68.2.138>
- Shrestha RK, Lal R (2008) Land use impacts on physical properties of 28 years old reclaimed mine soils in Ohio. *Plant Soil* 306(1): 249-260. <https://doi.org/10.1007/s11104-008-9578-4>
- Singh MK, Ghoshal N (2014) Variation in soil microbial biomass in the dry tropics: impact of land-use change. *Soil Res* 52(3): 299-306. <https://doi.org/10.1071/SR13265>
- Six J, Elliott ET, Paustian K (2000) Soil structure and soil organic matter II. A normalized stability index and the effect of mineralogy. *Soil Sci Soc Am J* 64(3): 1042-1049. <https://doi.org/10.2136/sssaj2000.6431042x>
- Su YY, Li P, Li ZB, et al. (2017) Effects of slope vegetation patterns on energy regulation and water-sediment response relations in slope-gully system. *J Soil Water Conserv* 31(5): 32-39.
- Tang JL, Cheng XQ, Zhu B, et al. (2015) Rainfall and Tillage Impacts on Soil Erosion of Sloping Cropland with Subtropical Monsoon Climate-A Case Study in Hilly Purple Soil area, China. *J Mt Sci* 12(001): 134-144. <https://doi.org/10.1007/s11629-014-3241-8>
- Tian GM, Wang FE, Chen YX, et al. (2003) Effect of different vegetation systems on soil erosion and soil nutrients in red soil region of southeastern China. *Soil circle* 13(2): 121-128. <https://doi.org/10.1023/A:1023354109910>
- Tisdall JM, OADES JM (1982) Organic matter and water-stable aggregates in soils. *Eur J Soil Sci* 33(2): 141-163. <https://doi.org/10.1111/j.1365-2389.1982.tb01755.x>
- Tu AG, Xie SH, Li Y, et al. (2019) Analysis of erosive rainfall distribution and sediment yield on long-term field monitoring sloping bare land of red soil. *Trans Chin Soc Agric Eng* 35(7): 7. (In Chinese) <https://doi.org/10.11975/j.issn.1002-6819.2019.07.016>
- Wagner S, Cattle SR, Scholten T (2010) Soil-aggregate formation as influenced by clay content and organic-matter amendment. *J Plant Nutr Soil Sci* 170(1): 173-180. <https://doi.org/10.1002/jpln.200521732>
- Wang JY, Deng YS, Li DY, et al. (2022) Soil aggregate stability and its response to overland flow in successive Eucalyptus plantations in subtropical China. *Sci Total Environ* 807: 151000. <https://doi.org/10.1016/j.scitotenv.2021.151000>
- Wang JG, Yang W, Yu B, et al. (2016) Estimating the influence of related soil properties on macro- and micro-aggregate stability in ultisols of south-central China. *Catena* 137: 545-553. <https://doi.org/10.1016/j.catena.2015.11.001>
- Wang K, Wang HJ, Shi XZ, et al. (2009) Landscape analysis of dynamic soil erosion in Subtropical China: A case study in Xingguo County, Jiangxi Province. *Soil Tillage Res* 105(2): 313-321. <https://doi.org/10.1016/j.still.2008.08.013>
- Wang SS, Huang XZ, Shi DM, et al. (2013a) Study on soil aggregates stability of mulberry ridge in Rocky Desertification based on Le Bissonnais method. *Acta Ecologica Sinica* 33(18): 5589-5598. (In Chinese) <https://doi.org/10.5846/stxb201305070977>
- Wang YL, Wang Y, Li LY, et al. (2013b) Composition characteristic of soil aggregates and their stability in red soils as affected by the soil parent materials and land use types. *Chin J Soil Sci* (04): 776-785. (In Chinese)
- Wei LJ, Bin LZ (2002) Advance in Soil Aggregate Study. *Res Soil Water Conserv* (1): 81-85. (In Chinese) <https://doi.org/10.3969/j.issn.1005-3409.2002.01.020>
- Wu XL, Cai CF, Wang JG, et al. (2016) Spatial variations of aggregate stability in relation to sesquioxides for zonal soils, South-central China. *Soil Tillage Res* 157: 11-22. <https://doi.org/10.1016/j.still.2015.11.005>
- Xiao SY, Shu YG (2021) Effects of land use patterns on soil water stable aggregates in Karst Canyon Area. *J Irrig Drain Eng* 40(04): 73-79. <https://doi.org/10.13522/j.cnki.gggs.2020600>
- Xu QG, Xi BD, Shen ZY, et al. (2007) Effects of farming practices on soil erosion and nutrient loss in the three-George reservoir area. *J Ecol Rural Environ* 23(3): 41-45. (In Chinese) <https://doi.org/10.3969/j.issn.1673-4831.2007.03.009>
- Yan FL, Shi ZH, Li ZX, et al. (2008) Estimating interrill soil erosion from aggregate stability of Ultisols in subtropical China. *Soil Tillage Res* 100(1-2): 34-41. <https://doi.org/10.1016/j.still.2008.04.006>
- Yang D, Kanae S, Oki T, et al. (2003) Global potential soil erosion with reference to land use and climate changes. *Hydrol Process* 17(14): 2913-2928. <https://doi.org/10.1002/hyp.1441>
- Yang YS, Xie JS, Sheng H, et al. (2009) The impact of land use/cover change on storage and quality of soil organic carbon in midsubtropical mountainous area of southern China. *J Geogr Sci* 19(1): 49-57. <https://doi.org/10.1007/s11442-009-0049-5>
- Ye C, Guo ZL, Li ZX, et al. (2017) The effect of Bahiagrass roots on soil erosion resistance of Aquilts in subtropical China. *Geomorphology* 285: 82-93. <https://doi.org/10.1016/j.geomorph.2017.02.003>
- Yu QZ, Shi MZ (1990) A Preliminary Report of Study on Soil Anti-erodibility of Mixture-planted Forest in Semiarid Loess Hilly Gully Region. *Bull Soil Water Conserv* 05. (In Chinese)
- Zeng QC, Darboux F, Man C, et al. (2018) Soil aggregate stability under different rain conditions for three vegetation types on the Loess Plateau (China). *Catena* 167: 276-283. <https://doi.org/10.1016/j.catena.2018.05.009>
- Zhang B, Horn R (2001) Mechanisms of aggregate stabilization in Ultisols from subtropical China. *Geoderma* 99(1-2): 123-145. [https://doi.org/10.1016/S0016-7061\(00\)00069-0](https://doi.org/10.1016/S0016-7061(00)00069-0)
- Zhang JB, Song CC (2004) Effects of different land-use on soil physical-chemical properties in the Sanjiang Plain. *Chin J Soil Sci* 35(3): 371-373. (In Chinese) [https://doi.org/10.1300/J064v24n01\\_09](https://doi.org/10.1300/J064v24n01_09)
- Zhang L, Luo TX, Deng KM, et al. (2004) Biomass and net primary productivity of secondary evergreen broadleaved forest in Huangmian Forest Farm, Guangxi. *Chin J Appl Ecol* 15(11): 2029. (In Chinese)
- Zhang MK, Han CC (2000) On antierodibility of hilly soils in Zhejiang Province. *Acta Agriculturae Zhejiangensis* 12(1): 25-30. (In Chinese)
- Zhang MK, He ZL, Chen GC, et al. (1996) Formation and water stability of aggregates in red soils as affected by organic matter. *Pedosphere* 6(1): 39-45. <https://doi.org/10.2136/sssaj2000.6441479x>
- Zhang Z, Liu T, Wu ZH (2008) Management, Utilization and Economic Effect Analysis of Eucalypt Plantation in Huangmian Forest Farm of Guangxi. *Eucalypt Science and Technology* 2. (In Chinese) <https://doi.org/10.3969/j.issn.1674-3172.2008.02.006>
- Zhang Z, Wei CF, Xie DT, et al. (2008) Effects of land use patterns on soil aggregate stability in Sichuan Basin, China. *Particology* 6(3): 157-166. <https://doi.org/10.1016/j.partic.2008.03.001>
- Zheng ZC, Li TX, Zhang XZ, et al. (2009) Study on the composition and stability of soil aggregates under different land use. *J Soil Water Conserv* 23(5): 228-231. <https://doi.org/10.3321/j.issn:1009-2242.2009.05.049>